Physical Oceanography - UNAM, Mexico
Lecture 2: The equations of Ocean Circulation and Ocean Modelling

Robin Waldman

September 4th, 2018

Contact :
CNRM, Météo France - CNRS
+33561079336
robin.waldman@meteo.fr

Contents

1 The equations of Ocean Circulation

The equations of ocean circulation are the core of ocean modelling. They are "the truth" of ocean models and despite their limited number of variables, they contain a large wealth of physical processes.

1.1 The fundamental laws of conservation in the ocean

The oceanic circulation can be comprehensively described by formulating the conservation of mass, momentum, heat and salt and an equation of state relating thermodynamic variables.

1.1.1 Conservation of mass: continuity

The mass continuity equation states that in the absence of any mass source, the fluid mass is conserved. Let us consider a control volume of zonal, meridional and vertical sizes δx, δy and δz and of density ρ on a fixed Cartesian coordinate system $(\mathbf{i}, \mathbf{j}, \mathbf{k})$ attached to the ground. Its mass conservation writes as:

$$\begin{aligned} \frac{d(\rho\delta x\delta y\delta z)}{dt} &= 0 \\ &= \delta x\delta y\delta z\frac{d\rho}{dt} + \rho(\delta y\delta z\frac{d\delta x}{dt} + \delta x\delta z\frac{d\delta y}{dt} + \delta x\delta y\frac{d\delta z}{dt}) \\ &= \delta x\delta y\delta z\frac{d\rho}{dt} + \rho(\delta y\delta z\delta u + \delta x\delta z\delta v + \delta x\delta y\delta w) \end{aligned}$$

with $\frac{d}{dt}$ the Lagrangian (or total) derivative operator, $\mathbf{u} = (u, v, w)$ the velocity vector. Hence dividing by $\delta x\delta y\delta z$ yields the volumic mass conservation equation:

$$\begin{aligned} \frac{d\rho}{dt} + \rho(\frac{\partial u}{\partial x} + \frac{\partial v}{\partial y} + \frac{\partial w}{\partial z}) &= 0 \\ \Longleftrightarrow \frac{d\rho}{dt} + \rho\boldsymbol{\nabla}.\mathbf{v} &= 0 \end{aligned}$$

with $\boldsymbol{\nabla} = (\frac{\partial}{\partial x}, \frac{\partial}{\partial y}, \frac{\partial}{\partial z})$ the space derivative operator.

In the ocean we make the Boussinesq approximation which states that relative density variations are small. With $\rho(x,y,z,t) = \rho_0 + \rho'(x,y,z,t)$ and $\rho' << \rho_0$, the continuity equation becomes:

$$\begin{aligned} \frac{d\rho'}{dt} + (\rho_0 + \rho')\boldsymbol{\nabla}.\mathbf{v} \simeq \rho_0\boldsymbol{\nabla}.\mathbf{v} &= 0 \\ \Longleftrightarrow \boldsymbol{\nabla}.\mathbf{v} &= 0 \end{aligned}$$

Hence to a very good approximation, oceanic currents are non-divergent. Note that the same results are obtained with the stronger and unnecessary hypothesis of incompressibility.

1.1.2 Conservation of momentum: Newton's 2nd law in a rotating frame

Newton's 2nd law states that the Lagrangian evolution of momentum is determined by the sum of external (gravity) and body (pressure and friction) forces. We first write the relation between

Lagrangian and Eulerian time derivatives by writing the chain rule of differenciation:

$$\begin{aligned}
\delta\mathbf{u} &= \frac{\partial \mathbf{u}}{\partial t}\delta t + \frac{\partial \mathbf{u}}{\partial x}\delta x + \frac{\partial \mathbf{u}}{\partial y}\delta y + \frac{\partial \mathbf{u}}{\partial z}\delta z \\
\Longleftrightarrow \frac{d\mathbf{u}}{dt} &= \frac{\partial \mathbf{u}}{\partial t}\frac{dt}{dt} + \frac{\partial \mathbf{u}}{\partial x}\frac{dx}{dt} + \frac{\partial \mathbf{u}}{\partial y}\frac{dy}{dt} + \frac{\partial \mathbf{u}}{\partial z}\frac{dz}{dt} \\
&= \frac{\partial \mathbf{u}}{\partial t} + \frac{\partial \mathbf{u}}{\partial x}u + \frac{\partial \mathbf{u}}{\partial y}v + \frac{\partial \mathbf{u}}{\partial z}w \\
&= \frac{\partial \mathbf{u}}{\partial t} + (\mathbf{u}.\boldsymbol{\nabla})\mathbf{u}
\end{aligned}$$

with $\frac{\partial \mathbf{u}}{\partial t}$ the Eulerian (or local) derivative being a far easier quantity to observe and model.

Going back to the control volume (see Fig.1.1), the zonal pressure force exerted on the western and eastern faces is:

$$F_{Px} = (P(x-\delta x) - P(x))\delta y \delta z$$

hence the volumic zonal pressure force is:

$$\frac{F_{Px}}{\delta x \delta y \delta z} = -\frac{\partial P}{\partial x}$$

and generalizing to other spatial dimensions:

$$\frac{\mathbf{F_P}}{\delta x \delta y \delta z} = -\boldsymbol{\nabla} P$$

As for friction $\boldsymbol{F_\tau}$, Newton's law of viscosity gives for a Boussinesq (or incompressible) Newtonian fluid:

$$\tau_{ij} = +\nu\rho(\frac{\partial u_j}{\partial x_i} + \frac{\partial u_i}{\partial x_j})$$

with τ_{ij} the viscous stress exerted over the coordinate i on velocity component j, $x_i, x_j = (x, y, z)$, $u_i, u_j = (u, v, w)$ and $\nu = 8.9 \times 10^{-7} m^2/s$ the water kinematic viscosity. The second term vanishes in a Boussinesq (or incompressible) fluid, hence it is neglected in the following. On the control volume, the zonal friction force is:

$$\begin{aligned}
F_{\tau x} &= (-\tau_{xx}(x-\delta x) + \tau_{xx}(x))\delta y \delta z + (-\tau_{yx}(y-\delta y) + \tau_{yx}(y))\delta x \delta z + (-\tau_{zx}(z-\delta z) + \tau_{zx}(z))\delta x \delta y \\
&= -\nu\rho\left[\frac{\partial}{\partial x}(x-\delta x)\delta y \delta z + \frac{\partial}{\partial y}(y-\delta y)\delta x \delta z + \frac{\partial}{\partial z}(z-\delta z)\delta x \delta y - \frac{\partial}{\partial x}(x)\delta y \delta z + \frac{\partial}{\partial y}(y)\delta x \delta z + \frac{\partial}{\partial z}(z)\delta x \delta y\right]u \\
&= +\nu\rho(\frac{\partial^2}{\partial x^2} + \frac{\partial^2}{\partial y^2} + \frac{\partial^2}{\partial z^2})u\delta x \delta y \delta z \\
&= +\nu\rho\Delta u \delta x \delta y \delta z
\end{aligned}$$

with $\Delta = \boldsymbol{\nabla}^2$ the Laplacian operator. Hence on the volume control over the three dimensions, the volumic friction force is:

$$\frac{\mathbf{F}_\tau}{\delta x \delta y \delta z} = +\nu\rho\Delta\mathbf{u}$$

Finally, Newton's second law writes on the volume control as:

$$\begin{aligned}
\rho\delta x \delta y \delta z(\frac{\partial \mathbf{u}}{\partial t} + (\mathbf{u}.\boldsymbol{\nabla})\mathbf{u}) &= \delta x \delta y \delta z(-\boldsymbol{\nabla} P + \nu\rho\Delta u - \rho g\mathbf{k}) \\
\Longleftrightarrow \frac{\partial \mathbf{u}}{\partial t} + (\mathbf{u}.\boldsymbol{\nabla})\mathbf{u} &= -\frac{1}{\rho}\boldsymbol{\nabla} P + \nu\Delta\mathbf{u} - g\mathbf{k}
\end{aligned}$$

with $g = 9.81 m/s^2$ the gravity acceleration and $\mathbf{k}$ the vertical unit vector. This last equation is the conservation of specific (or massic) momentum, that is velocities. However it is usually unproperly named the momentum conservation equation.

The vertical momentum equation can be simplified by noting that the ocean is to a very good approximation under hydrostatic balance, dominated by the vertical pressure and gravity forces:

$$\frac{\partial P}{\partial z} = -\rho g$$

The Boussinesq approximation also simplifies the momentum equations. It involves hydrostatic pressure, and the so-called second Boussinesq hypothesis states that $P = P_0 + P'$ with $P' << P_0$ as a consequence of $\rho' << \rho_0$. We write the volumic momentum equations with respect to a reference state at rest with $\frac{\partial P_0}{\partial z} = -\rho_0 g$:

$$\begin{aligned}
(\rho_0 + \rho')(\frac{\partial \mathbf{u_h'}}{\partial t} + (\mathbf{u}'.\mathbf{\nabla})\mathbf{u_h'}) &= -\mathbf{\nabla} P' + \nu(\rho_0 + \rho')\Delta \mathbf{u_h'} - \rho' g \mathbf{k} \\
\Longrightarrow \rho_0(\frac{\partial \mathbf{u_h'}}{\partial t} + (\mathbf{u}'.\mathbf{\nabla})\mathbf{u_h'}) &= -\mathbf{\nabla} P' + \nu\rho_0\Delta \mathbf{u_h'} - \rho' g \mathbf{k} \\
\Longrightarrow \frac{\partial \mathbf{u_h'}}{\partial t} + (\mathbf{u}'.\mathbf{\nabla})\mathbf{u_h'} &= -\frac{1}{\rho_0}\mathbf{\nabla} P' + \nu\Delta \mathbf{u_h'} - \frac{\rho'}{\rho_0} g \mathbf{k}
\end{aligned}$$

by assuming second-order terms on perturbations small. We can define $b = -\frac{\rho'}{\rho_0}g$ the buoyancy acceleration. It represents the effect of gravity on the stratified water column and thanks to the Boussinesq approximation, it is the only means by which the thermodynamics (active tracers temperature and salinity) impacts the dynamics (velocities) of ocean circulation. Hence the total momentum equation (reference plus perturbation) writes as:

$$\Longrightarrow \frac{\partial \mathbf{u_h}}{\partial t} + (\mathbf{u}.\mathbf{\nabla})\mathbf{u_h} = -\frac{1}{\rho_0}\mathbf{\nabla} P + \nu\Delta \mathbf{u_h} - \frac{\rho'}{\rho_0} g \mathbf{k}$$

with $\mathbf{u_h} = (u, v, 0)$ the horizontal velocity vector.

For geophysical fluids, several contributions arise from the Earth's rotation and its spherical shape. Fist on the plane Cartesian coordinates, two pseudo-forces arise from the Earth's rotation: the Coriolis and centrifugal accelerations. Second on the spherical coordinates, additional correction terms accounting for the Earth's curvature arise in the momentum equations: the metric (or curvature) terms. Although global numerical models are naturally written in spherical coordinates, most oceanic problems can be analyzed in the much simpler local Cartesian coordinates, the metric terms having a weak contribution to the momentum equations. We will henceforth limit the analysis to the Cartesian plane.

The Coriolis and centrifugal accelerations arise from the Earth's rotation inducing an acceleration in the local Cartesian coordinate system with respect to reference, non-rotating, coordinates. We consider the location of a water parcel $\mathbf{r}$ in an absolute non-rotating frame centered at the Earth's core. Its material evolution in the absolute frame is related to that in the relative local coordinates by the following relation:

$$(\frac{d\mathbf{r}}{dt})_A = (\frac{d\mathbf{r}}{dt})_R + \mathbf{\Omega} \times \mathbf{r} \iff \mathbf{u_A} = \mathbf{u_R} + \mathbf{\Omega} \times \mathbf{r}$$

with $\Omega = 7.29 \times 10^{-5} rad/s$ the Earth's angular velocity. A second derivation yields the correspondence of accelerations:

$$(\frac{d\mathbf{u_R}}{dt})_A = (\frac{d\mathbf{u_R}}{dt})_R + \mathbf{\Omega} \times \mathbf{u_R}$$

and with:

$$\begin{aligned}
(\frac{d\mathbf{u_R}}{dt})_A &= (\frac{d\mathbf{u_A}}{dt})_A - \frac{d}{dt}(\mathbf{\Omega}\times\mathbf{r})_A \\
&= (\frac{d\mathbf{u_A}}{dt})_A - \mathbf{\Omega}\times(\frac{d\mathbf{r}}{dt})_A \\
&= (\frac{d\mathbf{u_A}}{dt})_A - \mathbf{\Omega}\times(\mathbf{u_R}+\mathbf{\Omega}\times\mathbf{r})
\end{aligned}$$

we have:

$$(\frac{d\mathbf{u_R}}{dt})_R = (\frac{d\mathbf{u_A}}{dt})_A - 2\mathbf{\Omega}\times\mathbf{u_R} - \mathbf{\Omega}\times\mathbf{\Omega}\times\mathbf{r}$$

The first apparent force on the local rotating frame is the Coriolis acceleration, the second one being the centrifugal acceleration. The Coriolis acceleration can be written in terms of the Coriolis parameter $f = 2\Omega sin(\phi)$ (with ϕ the latitude) as : $2\mathbf{\Omega}\times\mathbf{u_R} = (-fu_R, +fv_R, 0)$. We have neglected the horizontal Coriolis acceleration (with $w << u, v$ and the hydrostatic assumption). The centrifugal acceleration is mostly vertical and compensated for by the Earth's deformation at low latitudes. We hence include it in an effective gravity force defined as:

$$\mathbf{g}^* = \mathbf{g}+\mathbf{\Omega}\times\mathbf{\Omega}\times\mathbf{r} \simeq -g^*\mathbf{k}$$

with $g^* = 9.81m/s^2$.

We finally obtain the following momentum equations under the hypotheses of Boussinesq, hydrostatism, tangent plane and the neglect of small terms related to the Earth's rotation:

$$\frac{\partial\mathbf{u_h}}{\partial t} + (\mathbf{u}.\mathbf{\nabla})\mathbf{u_h} + f\mathbf{k}\times\mathbf{u_h} = -\frac{1}{\rho_0}\mathbf{\nabla}P + \nu\Delta\mathbf{u_h} - g^*\mathbf{k}$$

1.1.3 Conservation of heat

Similarly to the conservation of mass over the control volume (see Fig.1.2), we deduce from the first law of thermodynamics the conservation of heat (or more precisely of potential temperature) as:

$$\frac{\partial\theta}{\partial t} + (\mathbf{u}.\mathbf{\nabla})\theta = \nu_T\Delta\theta + \frac{1}{\rho_0 c_w}\dot{\Theta}$$

with $\nu_T = 1.37\times10^{-7}m^2/s$ the thermal diffusivity of water, $c_w = 3993J/K/kg$ the water heat capacity, $\dot{\Theta}$ (in W/m^3) sources and sinks of heat and θ the seawater potential temperature. Potential temperature is defined as the temperature corrected from pressure effects, that is the temperature that the water parcel would have if uplifted adiabatically to surface. Due to the limited compressibility of sea water, the effect of pressure only induces a limited correction to θ. $\dot{\Theta}$ represents air-sea heat exchanges (and ice formation/fusion in the presence of sea ice).

1.1.4 The equation of state for seawater

Unlike the atmosphere, we do not dispose of an analytical equation relating density ρ to the other thermodynamic variables of ocean circulation. This simplifies the mathematical analysis of ocean thermodynamics, precisely because we have a more limited knowledge about it. Ocean models use an empirical 78-member polynomial function of salinity, potential temperature and pressure to deduce seawater density. Density cannot be assumed linear in θ, S and P (see Fig.1.3): in particular the thermal expansion of seawater varies typically between $-\alpha_\theta\rho = \frac{\partial\rho}{\partial\theta} \sim -0.05kg/m^3/°C$ for $\theta = 0°C$ and $-\alpha_\theta\rho \sim -0.35kg/m^3/°C$ for $\theta = 30°C$ with α_θ the thermal expansion coefficient

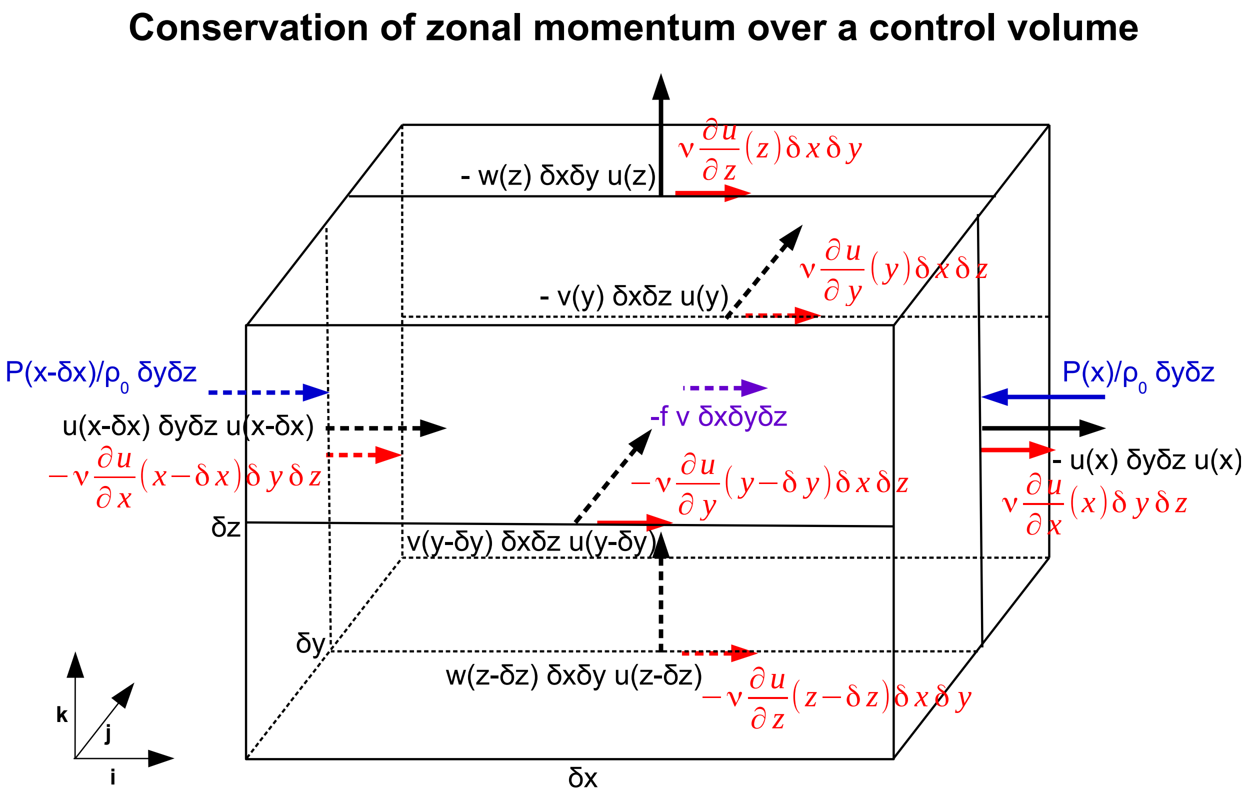

Figure 1.1: Conservation of zonal specific (massic) momentum over a control volume: advection (black), viscous forces (red), pressure forces (blue) and Coriolis acceleration (purple).

of seawater, for $S = 35$ ‰ and $P = P_a$. A reasonable formula is given by the inclusion of two second-order terms accounting for the main nonlinearities of density: cabbeling and thermobaricity. Cabbeling is the systematic densification of seawater by mixing, and thermobaricity is the small dependency of α_θ on pressure. The equation writes for the specific volume $v = \frac{1}{\rho}$:

$$v = v_0\left[1+\alpha_\theta(1+\gamma^* P)(\theta-\theta_0)+\alpha^*_\theta(\theta-\theta_0)^2-\beta_S(S-S_0)-\beta_P(P-P_0)\right]$$

with (v_0,θ_0,S_0,P_0) a reference state, $\beta = \frac{1}{\rho}\frac{\partial\rho}{\partial S}$ the haline contraction coefficient, $\beta_P = \frac{1}{\rho}\frac{\partial\rho}{\partial P}$ the compressibility coefficient, $\alpha^*_\theta = -\frac{1}{\rho}\frac{\partial^2\rho}{\partial\theta^2}$ the second thermal expansion (or cabbeling) coefficient and $\gamma^* = \frac{\partial\alpha_\theta}{\partial P}$ the thermobaric parameter.

The nonlinearity of seawater with respect to θ and S has important consequences. First although density is conserved as θ and S are, its conservation equation is complicated by the involvement of nonlinear terms, so that it is usually not explicitely formulated. Second, the ocean is usually more expanded from surface warming in the Tropics than contracted from surface cooling in the high latitudes, although the net heat flux is balanced. This average surface expansion of the global ocean, which would be equivalent to a heat imbalance of $Q_0 \sim +5W/m^2$, must be equilibrated otherwise the ocean would be ever expanding. It is indeed balanced by cabbeling which contracts the global ocean by mixing.

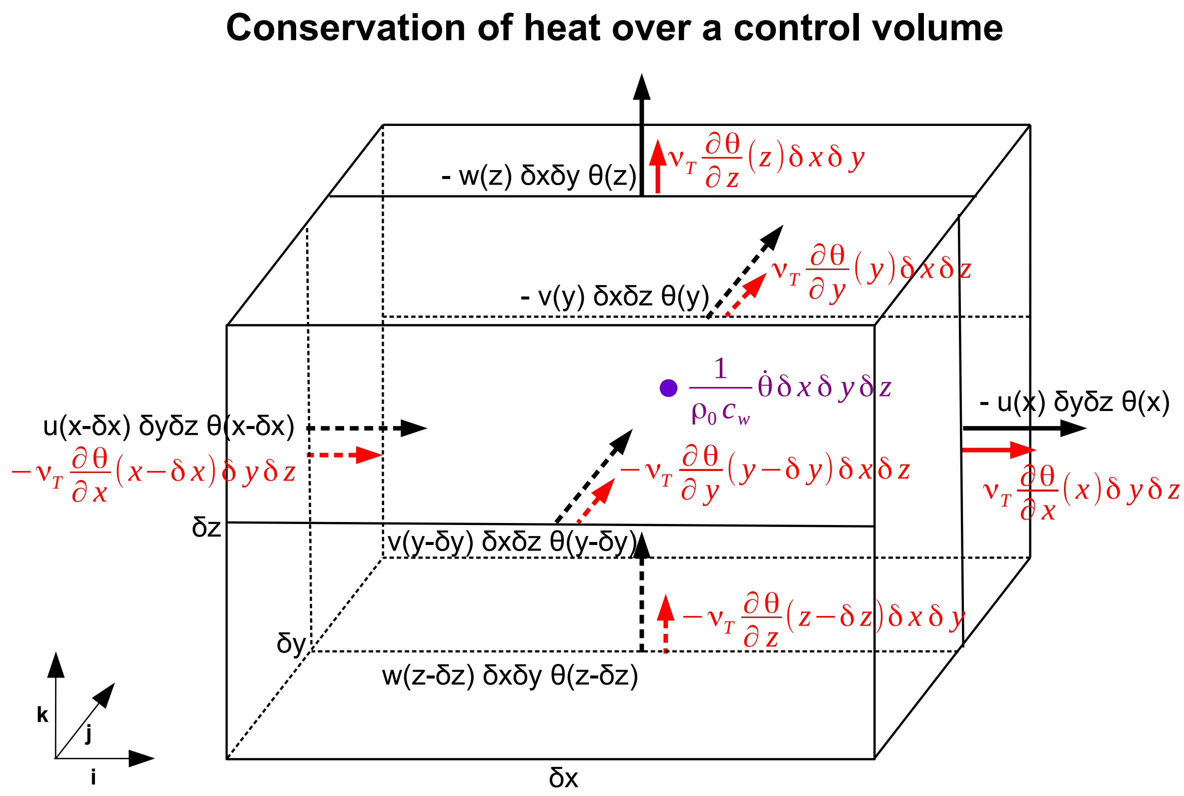

Figure 1.2: Conservation of heat over a control volume: advection (black), diffusion (red), and source/sink (purple).

For most oceanic applications, thermobaricity can be ignored, so that a potential density referenced at surface is the most commonly used density variable:

$$\sigma_0 = \rho(S, \theta, P = P_a) - 1000$$

1.1.5 Conservation of salt

The equation of state of seawater involves salinity, so that an equation for salinity must be formulated to close the system of equations of oceanic motion. Very similarly the the conservation of heat, the conservation of salt writes as:

$$\frac{\partial S}{\partial t} + (\mathbf{u}.\boldsymbol{\nabla})S = \nu_S \Delta S + \dot{S}$$

with $\nu_S \sim \nu_T/100$ the salt diffusivity of sea water, $\dot{S}$ (in $‰/s$) sources and sinks of salt and S in $‰$ or g/kg the concentration of dissolved salts. $\dot{S}$ represents air-sea water exchanges, river runoff and ice formation/fusion in the presence of sea ice. Indeed, the salinity of sea ice is typically $S \sim 5‰$ so that its formation is a source of salt (brine rejection) for sea water. We also note that salt diffusivity is by far lower than heat diffusivity, which can cause convective instabilities between water masses of different (θ, S) properties named salt fingering and convective layering. Those instabilities have a relatively minor role for mixing and ocean circulation.

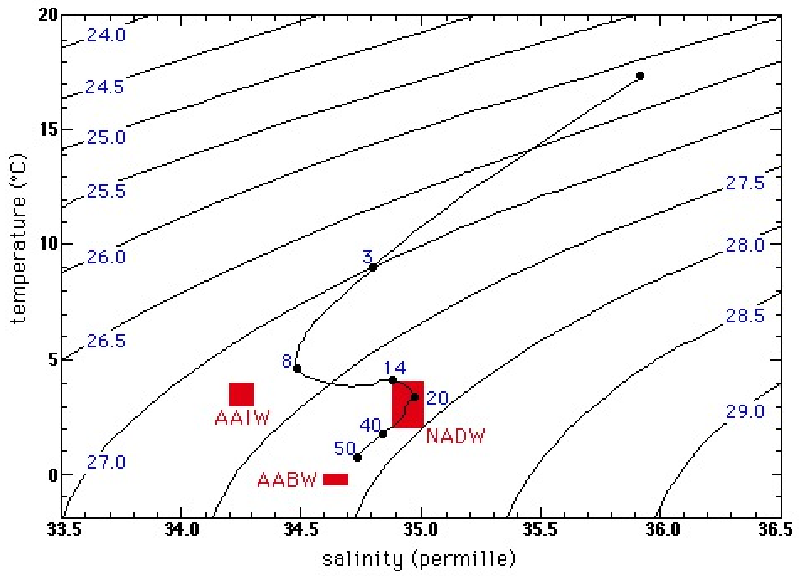

Figure 1.3: (θ, S) diagram of a hydrographic profile at $9°S$ in the Atlantic basin, from 150m to 5000m depth (depth in hm, main water masses in red, source: Benjamin Ménétrier's lecture). The curvature of isopycnal lines (iso-σ_0, black) illustrates the main nonlinearity of the seawater equation of state: cabbeling. Any mixing increases the density of the resulting water mass.

1.2 The simplified equations for the oceanic circulation

The geophysical and oceanic simplifications of the equations of motion yield a much simplified closed system of equations named the Boussinesq equations.

1.2.1 The Boussinesq equations

We first note that the default equations of motion constituting a closed system of equations for Newtonian fluids are named the Navier-Stokes Equations. For geophysical fluids, they are simplified (hydrostatic, shallow fluid and traditional approximation) to yield the Primitive Equations. In the ocean, the Boussinesq approximation simplifies them further, as we saw before, to yield the Boussinesq Equations. They write in the Cartesian coordinate frame (hence neglecting the curvature terms):

$$\begin{aligned}
\frac{\partial u}{\partial t}+u\frac{\partial u}{\partial x}+v\frac{\partial u}{\partial y}+w\frac{\partial u}{\partial z}-fv &= -\frac{1}{\rho_0}\frac{\partial P}{\partial x}+\nu(\frac{\partial^2}{\partial x^2}+\frac{\partial^2}{\partial y^2}+\frac{\partial^2}{\partial z^2})u \\
\frac{\partial v}{\partial t}+u\frac{\partial v}{\partial x}+v\frac{\partial v}{\partial y}v+w\frac{\partial v}{\partial z}+fu &= -\frac{1}{\rho_0}\frac{\partial P}{\partial y}+\nu(\frac{\partial^2}{\partial x^2}+\frac{\partial^2}{\partial y^2}+\frac{\partial^2}{\partial z^2})v \\
\frac{\partial P}{\partial z}=-\rho g^* \Longrightarrow P(z) &= \int_z^\eta -\rho g^* dz' + P_a \simeq \rho_0 g^* \eta + g^* \int_z^0 \rho dz' \\
\frac{\partial w}{\partial z}=-\frac{\partial u}{\partial x}-\frac{\partial v}{\partial y} \Longrightarrow w(z) &= -\int_{-H}^z (\frac{\partial u}{\partial x}+\frac{\partial v}{\partial y})dz' \\
\frac{\partial \theta}{\partial t}+u\frac{\partial \theta}{\partial x}+v\frac{\partial \theta}{\partial y}+w\frac{\partial \theta}{\partial z} &= \nu_T(\frac{\partial^2}{\partial x^2}+\frac{\partial^2}{\partial y^2}+\frac{\partial^2}{\partial z^2})\theta+\frac{1}{\rho_0 c_w}\dot{\Theta} \\
\frac{\partial S}{\partial t}+u\frac{\partial S}{\partial x}+v\frac{\partial S}{\partial y}+w\frac{\partial S}{\partial z} &= \nu_S(\frac{\partial^2}{\partial x^2}+\frac{\partial^2}{\partial y^2}+\frac{\partial^2}{\partial z^2})S+\dot{S} \\
\rho &= \rho(\theta,S,P_0(z))
\end{aligned}$$

with $H>0$ and η the ocean bottom depth (opposite to the bathymetry) and surface (dynamic sea level).

The vertical integration of the hydrostatic relation uses the surface dynamic boundary condition $P=P_a\simeq 0$ at $z=\eta$ as a constant of integration, P_a being usually neglected (except for storm surge and meteotsunami applications). However, its upper bound, the dynamic sea level η, is undetermined. To close the system of equations (currently 7 equations for 8 unknowns), we therefore need an equation for η. We obtain it from the vertical intrgration of continuity plus the surface and bottom kinematic boundary conditions. Indeed, sea level variations correspond to the water that accumulates or exits from the water column. The surface kinematic boundary condition is:

$$\frac{d}{dt}(\eta-z)_\eta = P+R-E \Longrightarrow \frac{\partial \eta}{\partial t} = -\mathbf{u_h}.\boldsymbol{\nabla}_h\eta + w(\eta)+P+R-E$$

with P, R and E the precipitation, river runoff and evaporation rates in m/s. The bottom kinematic boundary condition is:

$$\frac{d}{dt}(z+H)_{-H}=0 \Longrightarrow w(-H)=\frac{d}{dt}(-H)=-\mathbf{u_h}.\boldsymbol{\nabla}_h H$$

which expresses the no normal flow at bottom. Finally vertical integration of the continuity equation yields:

$$\int_{-H}^\eta \frac{\partial w}{\partial z}dz = w(\eta)-w(-H) = \frac{\partial \eta}{\partial t}+\mathbf{u_h}(\eta).\boldsymbol{\nabla}_h\eta - \mathbf{u_h}(-H).\boldsymbol{\nabla}_h(-H)$$

and

$$\int_{-H}^\eta -\boldsymbol{\nabla}_h.\mathbf{u_h}dz = -\boldsymbol{\nabla}_h.\int_{-H}^\eta \mathbf{u_h}dz + \mathbf{u_h}(\eta).\boldsymbol{\nabla}_h\eta - \mathbf{u_h}(-H).\boldsymbol{\nabla}_h(-H)$$

using Leibnitz's integration formula. It finally gives:

$$\frac{\partial \eta}{\partial t} = -\boldsymbol{\nabla}_h.\int_{-H}^\eta \mathbf{u_h}dz + P+R-E$$

Hence the dynamic sea level is set by surface water exchanges and by vertically-integrated horizontal convergence. This is the 8th and last equation of the Boussinesq equation system.

The Boussinesq approximations have permitted to filter out sound waves whose very large velocities $c_s \simeq 1500m/s$ would have been a major issue for the numerical resolution of oceanic circulation. However, it still includes one type of fast waves that will require specific numerical treatments: external gravity waves with $c_g=\sqrt{gH}\sim 200m/s$. We will come back to this in the next section.

1.2.2 The Reynolds-Averaged Boussinesq equations

In ocean modelling, we do not generally resolve all the scales of motions, ranging from the global scale to the millimetric scale of diffusion. The Reynolds number for large-scale motions is $Re = \frac{UL}{\nu} \sim 10^{11}$, meaning that the smallest scales to be resolved (millimetric diffusion) are one hundred billion times smaller than the largest scales to be resolved (basin scales). In terms of modelling, such a range of scales would require to resolve 10^4 moles of grid points, which will remain impossible for a long time. Hence a formal separation must be performed on the equations of motion to identify the influence of small-scale unresolved motion on the large-scale resolved motion.

A Reynolds average is hence performed on the Boussinesq system of equations. We decompose all variables into a mean and a perturbation, e.g. $\mathbf{u} = \overline{\mathbf{u}} + \mathbf{u}'$. Reynolds assumed the mean to be an ensemble average, but for numerical modelling we do the ergodic hypothesis which assimilates ensemble to spatio-temporal means, so that we consider $\overline{\mathbf{u}}$ as the large-scale (resolved) variable and $\mathbf{u}'$ as the small-scale (unresolved and to be parametrized) variable. Note that this is a strong hypothesis that fragilizes the current ocean modelling framework. Hence, under Reynolds's hypotheses on his mean operator (linearity, commutativity and indempotency), all non-linear terms of the Boussinesq equations are modified, the linear ones remaining unchanged. For instance, in the zonal momentum equation, the time derivative is linear so that:

$$\overline{\frac{\partial u}{\partial t}} = \overline{\frac{\partial(\overline{u}+u')}{\partial t}} = \overline{\frac{\partial \overline{u}}{\partial t} + \frac{\partial u'}{\partial t}} = \frac{\partial \overline{\overline{u}}}{\partial t} + \frac{\partial \overline{u'}}{\partial t} = \frac{\partial \overline{u}}{\partial t}$$

On the contrary, meridional advection is non-linear (second-order), so that:

$$\overline{v\frac{\partial u}{\partial y}} = \overline{(\overline{v}+v')\frac{\partial(\overline{u}+u')}{\partial y}} = \overline{\overline{v}\frac{\partial \overline{u}}{\partial y}} + \overline{\overline{v}\frac{\partial u'}{\partial y}} + \overline{v'\frac{\partial \overline{u}}{\partial y}} + \overline{v'\frac{\partial u'}{\partial y}} = \overline{v}\frac{\partial \overline{u}}{\partial y} + \overline{v}\frac{\partial \overline{u'}}{\partial y} + \overline{v'}\frac{\partial \overline{u}}{\partial y} + \overline{v'\frac{\partial u'}{\partial y}} = \overline{v}\frac{\partial \overline{u}}{\partial y} + \overline{v'\frac{\partial u'}{\partial y}}$$

We get a similar result for zonal and vertical advection, so that with the use of continuity we have (see Fig.1.4 for the illustration):

$$\overline{(\mathbf{u}.\boldsymbol{\nabla})u} = (\overline{\mathbf{u}}.\boldsymbol{\nabla})\overline{u} + \overline{(\mathbf{u}'.\boldsymbol{\nabla})u'} = (\overline{\mathbf{u}}.\boldsymbol{\nabla})\overline{u} + \boldsymbol{\nabla}.(\overline{\mathbf{u}'u'})$$

The second term is a turbulent (or eddy) transport contribution in the equation for the Reynolds-averaged zonal momentum $\overline{u}$. This means that the covariance of zonal velocity with each component of velocity at the turbulent (hence unresolved) scale induces a non-zero contribution to the momentum equation. Similarly for meridional velocity and for tracers θ and S we get:

$$\begin{aligned}
\overline{(\mathbf{u}.\boldsymbol{\nabla})v} &= (\overline{\mathbf{u}}.\boldsymbol{\nabla})\overline{v} + \boldsymbol{\nabla}.(\overline{\mathbf{u}'v'}) \\
\overline{(\mathbf{u}.\boldsymbol{\nabla})\theta} &= (\overline{\mathbf{u}}.\boldsymbol{\nabla})\overline{\theta} + \boldsymbol{\nabla}.(\overline{\mathbf{u}'\theta'}) \\
\overline{(\mathbf{u}.\boldsymbol{\nabla})S} &= (\overline{\mathbf{u}}.\boldsymbol{\nabla})\overline{S} + \boldsymbol{\nabla}.(\overline{\mathbf{u}'S'})
\end{aligned}$$

Hence a total of 12 additional transport terms appear in the conservation of horizontal momentum, heat and salt, which correspond to the divergence of the three-dimensional turbulent (or eddy) transports of u, v, θ and S. Those are actually 12 new variables for the system of equations which hence needs 12 new equations to be closed. In order to close the system, we must formulate an equation for each of those terms, which is called a closure hypothesis. The most common closure of turbulence is the introduction of turbulent diffusivities (see Fig.1.4). We assume just like molecular diffusion the flux-gradient relation so that each turbulent flux $\overline{\mathbf{u}'X'}$ (with X either u, v, θ or S) is proportional to the gradient of the Reynolds-averaged (resolved) quantity $\nabla\overline{X}$. More specifically, we separate vertical and horizontal eddy fluxes, the former being damped by gravity, and we pose:

$$\begin{aligned}
\overline{\mathbf{u_h}'X'} &= -\kappa_{hX}\boldsymbol{\nabla}_h\overline{X} \\
\overline{w'X'} &= -\kappa_{zX}\frac{\partial \overline{X}}{\partial z}
\end{aligned}$$

with κ_{hX} and κ_{zX} the horizontal and vertical eddy diffusivities for the variable X. Those diffusivities are several orders of magnitude larger than the molecular diffusivities in the momentum, temperature and salinity equations. Hence we obtain the Reynolds-averaged Boussinesq equations by simply replacing molecular by turbulent diffusivities and specifying that the equations are solved for the Reynolds-averaged quantities:

$$
\begin{aligned}
\frac{\partial \overline{\mathbf{u_h}}}{\partial t} + (\overline{\mathbf{u}}.\boldsymbol{\nabla})\overline{\mathbf{u_h}} + f\mathbf{k}\times\overline{\mathbf{u_h}} &= -\frac{1}{\rho_0}\boldsymbol{\nabla}_{\boldsymbol{h}}\overline{P} + \boldsymbol{\nabla}_{\boldsymbol{h}}.(\kappa_{hu}\boldsymbol{\nabla}_{\boldsymbol{h}})\overline{\mathbf{u_h}} + \frac{\partial}{\partial z}(\kappa_{zu}\frac{\partial \overline{\mathbf{u_h}}}{\partial z}) \\
\overline{P}(z) &= \rho_0 g\overline{\eta} + g\int_z^0 \overline{\rho}dz' \\
\overline{w}(z) &= -\int_{-H}^{z} \boldsymbol{\nabla}_{\boldsymbol{h}}.\overline{\mathbf{u_h}}dz' \\
\frac{\partial \overline{\eta}}{\partial t} &= -\boldsymbol{\nabla}_{\boldsymbol{h}}.\int_{-H}^{\eta} \overline{\mathbf{u_h}}dz + \overline{P} + \overline{R} - \overline{E} \\
\frac{\partial \overline{\theta}}{\partial t} + (\overline{\mathbf{u}}.\boldsymbol{\nabla})\overline{\theta} &= \boldsymbol{\nabla}_{\boldsymbol{h}}.(\kappa_{hT}\boldsymbol{\nabla}_{\boldsymbol{h}})\overline{\theta} + \frac{\partial}{\partial z}(\kappa_{zT}\frac{\partial \overline{\theta}}{\partial z}) + \frac{1}{\rho c_w}\overline{\dot{\Theta}} \\
\frac{\partial \overline{S}}{\partial t} + (\overline{\mathbf{u}}.\boldsymbol{\nabla})\overline{S} &= \boldsymbol{\nabla}_{\boldsymbol{h}}.(\kappa_{hS}\boldsymbol{\nabla}_{\boldsymbol{h}})\overline{S} + \frac{\partial}{\partial z}(\kappa_{zS}\frac{\partial \overline{S}}{\partial z}) + \overline{\dot{S}} \\
\overline{\rho} &= \overline{\rho}(\overline{\theta},\overline{S},\overline{P_0}(z))
\end{aligned}
$$

with the turbulent diffusivities varying spatially, contrary to their molecular counterpart. Note that we have technically neglected the turbulent (unresolved) tracer fluctuations ($\overline{\theta'^2}$, $\overline{S'^2}$, $\overline{\theta' S'}$ and higher-order terms) in the equation of state that could also have an impact on the Reynolds-averaged (resolved) density $\overline{\rho}$.

The Reynolds average sign above all variables of the equation system reminds us that it is far from describing the "truth" of the very turbulent ocean circulation. We make here the strong assumption that turbulence, which is an advective process, can be modelled as a diffusive process. In particular, we assume that turbulent fluxes are a function of the local large-scale variables (locality), that they are proportional to their gradients (flux-gradient relation), that they only flux the properties down this gradient (downgradient fluxes). We have also assumed that a deterministic relation exists between turbulent fluxes and the averaged quantities, although turbulent motion is chaotic and hence largely random by nature. However, all the wealth of unresolved turbulent processes (e.g. convection, shear instabilities, wave breaking, etc.) will have to enter into those turbulent diffusivities. This is why they are generally not constant and can have complex mathematical formulations. We will come back to this in the next section. In the following we will remove the Reynolds average sign for simplicity.

1.3 Dimensional analysis and leading-order balances

In the formulation of the momentum conservation, we have made a series of assumptions which derived from dimensional analysis. Let us come back to the full momentum equations to quantify the validity of these assumptions and identify the leading-order balances.

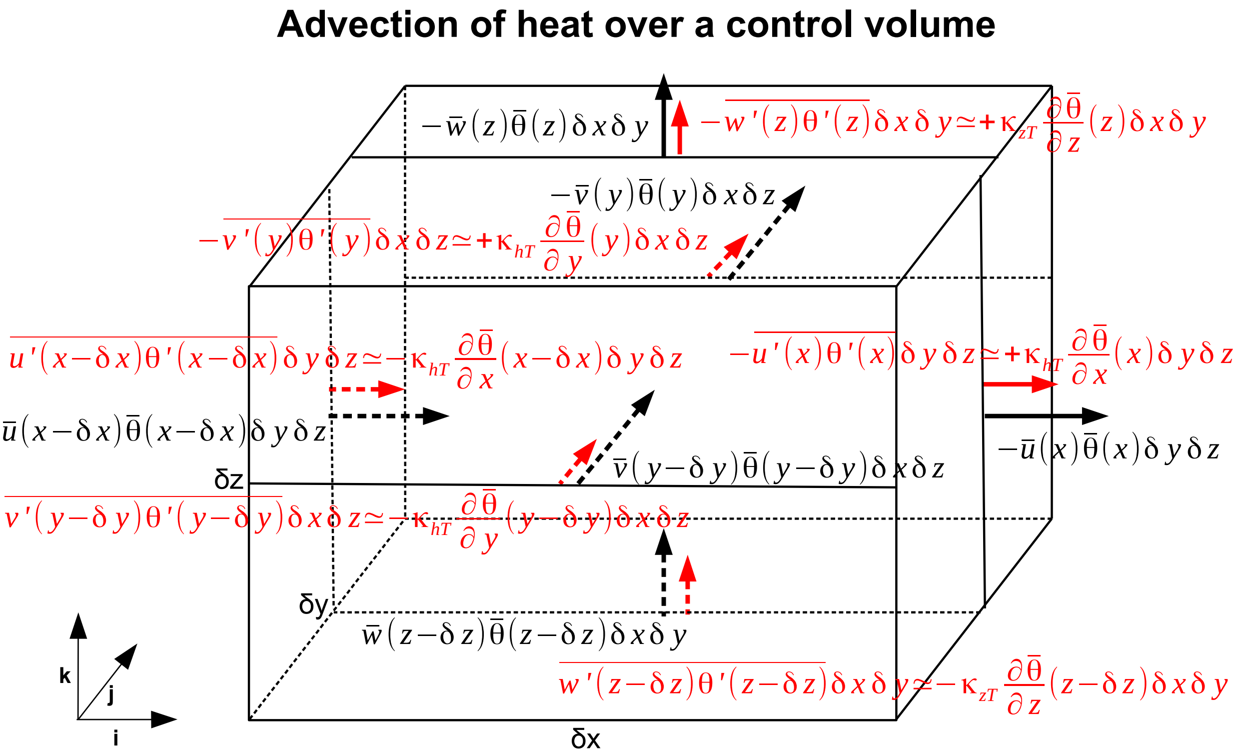

Figure 1.4: Heat advection over the control volume: mean (resolved, black) and turbulent (unresolved, red), the latter being parametrized as a so-called "turbulent diffusion".

1.3.1 Dimensional analysis

The full equations of motion are in a Cartesian coordinates frame:

$$
\begin{aligned}
\frac{Du}{Dt} - \frac{uv\tan(\phi)}{a} + \frac{uw}{a} &= -\frac{1}{\rho}\frac{\partial p}{\partial x} + 2\Omega v\sin(\phi) - 2\Omega w\cos(\phi) + \nu\Delta u \\
\frac{Dv}{Dt} - \frac{u^2\tan(\phi)}{a} + \frac{vw}{a} &= -\frac{1}{\rho}\frac{\partial p}{\partial y} - 2\Omega u\sin(\phi) + \nu\Delta v \\
\frac{Dw}{Dt} - \frac{u^2+v^2}{a} &= -\frac{1}{\rho}\frac{\partial p}{\partial z} + 2\Omega u\cos(\phi) - g^* + \nu\Delta w
\end{aligned}
$$

The additional terms on the left-hand side correspond to the Earth curvature (or metric) terms, and the additional terms involving Ω in the right-hand side are the horizontal Coriolis acceleration.

We are interested in large-scale motions of typical scales $L \sim 1000km$, $H \sim 1000m$ and $U \sim 0.1m/s$. We deduce from the continuity equation the typical vertical velocity scale: $W \sim \frac{H}{L}U = 0.1mm/s$. The characteristic timescale of those motions is hence: $T \sim \frac{L}{U} = 10^7 s \sim 1$ year. At mid-latitude $f_0 = 2\Omega sin(\phi) \simeq 2\Omega cos(\phi) \simeq 10^{-4}s^{-1}$. We also recall that the water kinematic viscosity scales as $\nu \sim 10^{-3}m^2/s$. We deduce Table1.1 and Table1.2 which list the order of magnitude of the acceleration caused by each term in the horizontal and vertical momentum equations.

The geostrophic and hydrostatic balances stand out to an excellent approximation as the leading-order balances in the equations of motion. The dimensional analysis allows to determine the typical horizontal and vertical variations of pressure: $\delta P_L \sim f_0 U \rho L \sim 10^4 Pa$ and $\delta P_H \sim \rho H g^* \sim 10^7 Pa$. Hence typical horizontal variations of the dynamic sea level are $\delta \eta_H \sim \delta P_H/(\rho_0 g^*) \sim 1m$.

The next order terms in the horizontal momentum equations are, in decreasing order of importance:

- The momentum trend and advection; however we note that turbulent advection can be strong enough to become a leading-order term in the surface layer (Ekman or convective layer) when $\kappa_{zu} U/H^2 \to 10^{-5}$;
- The non-Boussinesq contribution to the horizontal pressure gradient;
- The horizontal Coriolis acceleration;
- The main metric terms;
- The vertical molecular viscosity;
- The secondary metric terms;
- The horizontal molecular viscosity.

A striking result is the smallness of molecular viscosity. Indeed, the ocean is put into motion at the large scale, but an energetic analysis shows that this energy ultimately dissipates through molecular viscosity. Hence the turbulence of ocean circulation must find a route from the global energy input and the molecular energy sink.

Zonal	$\frac{Du}{Dt}$	$-\frac{uv\tan(\phi)}{a}$	$+\frac{uw}{a}$	$=$	$-\frac{1}{\rho_0}\frac{\partial p}{\partial x}$	$+\frac{\rho'}{\rho_0^2}\frac{\partial p}{\partial x}$	$+2\Omega v\sin(\phi)$	$-2\Omega w\cos(\phi)$	$+\nu\Delta u$
Meridional	$\frac{Dv}{Dt}$	$-\frac{u^2\tan(\phi)}{a}$	$+\frac{vw}{a}$	$=$	$-\frac{1}{\rho_0}\frac{\partial p}{\partial y}$	$+\frac{\rho'}{\rho_0^2}\frac{\partial p}{\partial y}$	$-2\Omega u\sin(\phi)$		$+\nu\Delta v$
OoM	U^2/L	U^2/a	UW/a		$\delta P_L/(\rho_0 L)$	$(\delta P_L\rho')/(\rho_0^2 L)$	$f_0 U$	$f_0 W$	$\nu U/H^2$
Value	10^{-8}	10^{-9}	10^{-12}		$? = 10^{-5}$	$?/1000 = 10^{-8}$	10^{-5}	10^{-8}	10^{-10}

Table 1.1: Orders of magnitude (OoM) for large-scale horizontal motion.

Vertical	$\frac{Dw}{Dt}$	$-\frac{u^2+v^2}{a}$	$=$	$-\frac{1}{\rho_0}\frac{\partial p}{\partial z}$	$+\frac{\rho'}{\rho_0^2}\frac{\partial p}{\partial z}$	$+2\Omega u\cos(\phi)$	$-g^*\frac{\rho_0}{\rho}$	$-g^*\frac{\rho'}{\rho}$	$+\nu\Delta w$
OoM	UW/L	U^2/a		$\delta P_H/(\rho_0 H)$	$\delta P_H\rho'/(\rho_0^2 H)$	$f_0 U$	g^*	$g^*\rho'/rho_0$	$\nu W/H^2$
Value	10^{-11}	10^{-9}		$? = 10$	$?/1000 = 10^{-2}$	10^{-5}	10	10^{-2}	10^{-13}

Table 1.2: Orders of magnitude (OoM) for large-scale vertical motion.

1.3.2 Zero-order: geostrophy, Ekman and hydrostatism

The geostrophic balance has already been introduced in Chapter 1. It writes as:

$$f\mathbf{k}\times\mathbf{u_g} = -\frac{1}{\rho_0}\boldsymbol{\nabla}_h P$$

with $\mathbf{u_g}$ horizontal geostrophic velocities. We can remark from the scaling analysis that this relation is even more true in the ocean than in the atmosphere, with the Rossby number $Ro = \frac{U}{fL} \sim 10^{-3}$ at the large-scale. This means that as noted above, the inertial terms (time derivative and advection) are one thousand times smaller than the pressure force and Coriolis acceleration at the large-scale. At the mesoscale, with $L \sim 50km$ and $U \sim 0.5m/s$ we still have $Ro \sim 0.1$, so that mesoscale eddies obey to quasi-geostrophic dynamics. Hence far from frictional boundary layers and the Equator, it is necessary to go down to the submesoscale $L \sim 1 - 10km$ for the flow to deviate significantly from geostrophy.

As noted above, within the frictional surface layer (or Ekman layer), vertical turbulent advection of momentum related to surface forcing can become dominant in the horizontal momentum equations, in which case we have:

$$f\mathbf{k} \times \mathbf{u_h} = -\frac{1}{\rho_0}\boldsymbol{\nabla}_h P + \frac{\partial}{\partial z}(\kappa_{zu}\frac{\partial \mathbf{u_h}}{\partial z})$$

or with the decomposition $\mathbf{u_h} = \mathbf{u_g} + \mathbf{u_E}$:

$$f\mathbf{k} \times \mathbf{u_E} = \frac{\partial}{\partial z}(\kappa_{zu}\frac{\partial \mathbf{u_E}}{\partial z})$$

We will come back to this balance in the following chapter. Finally, it is useful to note that the tendency term of the momentum equations $\frac{\partial \mathbf{u_h}}{\partial t}$, which permits to integrate forward in time the ocean circulation, is several orders of magnitude weaker than the leading-order terms. This means that although the horizontal momentum equations are prognostic (time-dependent), they mostly describe diagnostic (time-independent) balances between physical terms that equilibrate.

The hydrostatic relation has been posed early in this chapter. Indeed, its domain of validity is even larger than geostrophy with the next-order term one million times smaller than the pressure and gravity forces. Vertical velocity is hence named a diagnostic variable deduced from a time-independent equation (as are P and ρ), as opposed to the prognostic variables deduced from a time-dependent equation (as are u, v, η, θ and S). Vertical acceleration becomes significant in the perturbation analysis when $W \sim U \sim 0.1m/s$ and $L \sim 1m$, that is for fully developed 3-dimensional turbulence. In that case, it becomes of the same order of magnitude as the hydrostatic balance for the perturbations P' and ρ', which are the only contributions of P and ρ that are coupled with horizontal dynamics. This is in particular the case of convection which is filtered out of the equations by the hydrostatic assumption. This process, as many others, will have to be parametrized in the so-called eddy diffusivity coefficients κ_{zu}, κ_{zT} and κ_{zS}.

Exercise: transport across Drake Passage. Using the dynamical method with a level of no motion at 4000m depth and assuming a linear equation of state $\rho = \rho_0(-\alpha_\theta\theta + \beta_S S)$, estimate from the meridional hydrographic section (Fig.1.5) the mean surface velocity and the integral transport across the Drake passage. We have $\alpha_\theta \simeq 10^{-4}\ {}^\circ C^{-1}$, $\beta_S \simeq 10^{-3}‰^{-1}$, $f_0 \simeq -1 \times 10^{-4} s^{-1}$.

Solution: the dynamical method consists in retrieving geostrophic velocities from the vertical integration of the thermal wind relation, which uses both geostrophy and hydrostatism, from a reference level. The thermal wind relation writes as:

$$\begin{aligned}
\frac{\partial u_g}{\partial z} &= \frac{\partial}{\partial z}(-\frac{1}{f_0\rho_0}\frac{\partial P}{\partial y}) \\
&= -\frac{1}{f_0\rho_0}\frac{\partial}{\partial y}(\frac{\partial P}{\partial z}) \\
&= -\frac{1}{f_0\rho_0}\frac{\partial}{\partial y}(-\rho g) \\
&= +\frac{g}{f_0\rho_0}\frac{\partial \rho}{\partial y} \\
&= +\frac{g}{f_0}(-\alpha_\theta\frac{\partial \theta}{\partial y} + \beta_S\frac{\partial S}{\partial y})
\end{aligned}$$

Let us integrate this relation per layer of $\Delta z \sim 1000m$ height and over the width $\Delta y \simeq 500km$. We

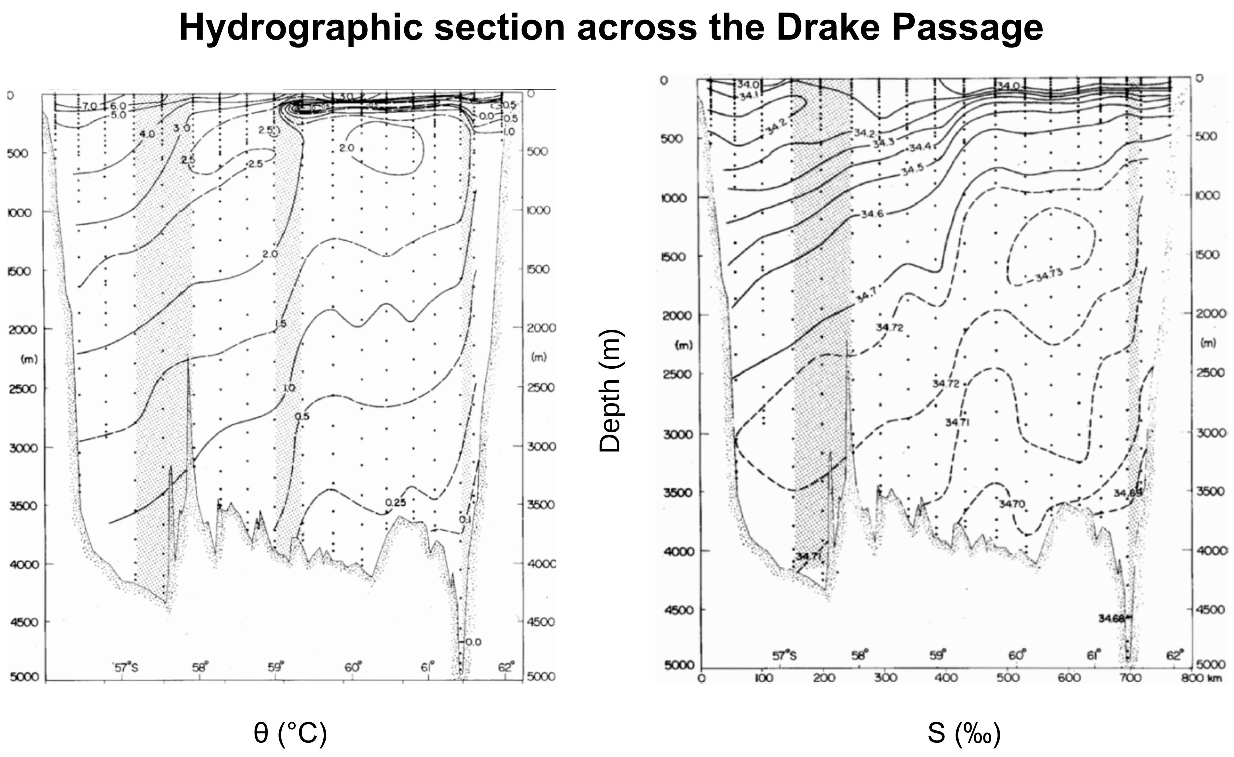

Figure 1.5: Hydrographic section across the Drake Passage (source: Helen Johnson's lecture). The dynamical method allows to estimate accurately transports with no direct velocity measurements.

read:

$$\begin{aligned}
\Delta\theta_{0-1000m} &\simeq +5^{\circ}C, \Delta S_{0-1000m} \simeq -0.2 \\
\Delta\theta_{1000-2000m} &\simeq +1.5^{\circ}C, \Delta S_{1000-2000m} \simeq -0.2 \\
\Delta\theta_{2000-3000m} &\simeq +1.5^{\circ}C, \Delta S_{2000-3000m} \simeq -0.02 \\
\Delta\theta_{3000-4000m} &\simeq +1^{\circ}C, \Delta S_{3000-4000m} \simeq +0.03
\end{aligned}$$

Hence we have:

$$\begin{aligned}
\Delta u_{3000-4000m} &= u_{3000m} = \frac{g\Delta z}{f_0 \Delta y}(-\alpha_\theta \Delta\theta_{3000-4000m} + \beta_S \Delta S_{3000-4000m}) \\
&\simeq -500 \times (-1 \times 10^{-4} + 0.03 \times 10^{-3}) \simeq +3.5 cm/s \\
u_{2000m} &= u_{3000m} + \Delta u_{2000-3000m} \\
&\simeq 0.035 - 500 \times (-1.5 \times 10^{-4} - 0.02 \times 10^{-3}) \simeq 12 cm/s \\
u_{1000m} &= u_{2000m} + \Delta u_{1000-2000m} \\
&\simeq 0.12 - 500 \times (-1.5 \times 10^{-4} - 0.2 \times 10^{-3}) \simeq 29.5 cm/s \\
u_{0m} &= u_{1000m} + \Delta u_{0-1000m} \\
&\simeq 0.295 - 500 \times (-5 \times 10^{-4} - 0.2 \times 10^{-3}) \simeq 64.5 cm/s
\end{aligned}$$

We can deduce the integral transport across Drake passage by integrating meridionally and verti-

cally those velocities:

$$\begin{aligned} T_{Drake} &\simeq \Delta y \Delta z (u_{4000m}/2 + u_{3000m} + u_{2000m} + u_{1000m} + u_{0m}/2) \\ &\simeq 5 \times 10^8 (0.035 + 0.12 + 0.295 + 0.645/2) \simeq 386 Sv \end{aligned}$$

This is the right order of magnitude for transports across the Drake Passage, although due to the numerical approximations it is overestimated by a factor $\sim 2-3$*. Those surface velocities and transports are among the most intense geostrophic currents found in the global ocean.*

2 Ocean modelling

Before the 1960's, only very simplified equations of motion were manipulated by oceanographers to understand the dynamics. Some of them had analytical solutions, which was extremely useful before the existence of computers. Obviously, the Boussinesq equations, which are a simplification of the Navier-Stokes equations, have no analytical solution so far, which is one of the seven "millennial problems". In the late 1960's, the first ocean models were developed and run on computers which resolved numerically the equations of motion.

Equations of motion within ocean models are essentially the same as the Reynolds-averaged Boussinesq equations presented before, with the following specificities:

- The coordinate system is not Cartesian but curvilinear (spherical) with horizontal axes that are not simply longitude and latitude.
- They are resolved over a finite number of grid cells and time steps, and hence must be discretized in time and space.
- A wide variety of lateral and vertical physical parametrizations can be introduced which all aim at modelling the unresolved turbulent motions.
- All boundary conditions (surface, lateral and bottom) must be specified for the equations to be solved in a given domain.

In the following we will mostly focus on NEMO model, which is arguably the most used large-scale ocean model in Europe. However, most of the considerations are general to ocean modelling.

2.1 Discretization

2.1.1 Time discretization

The equations for u, v, η, θ and S are prognostic, which allows to step forward in time the ocean circulation and to predict its future state. This means that the Boussinesq equations must be discretized in time. In NEMO model, it is done through the leapfrog scheme which writes as follows:

$$X(t+\delta t) = X(t-\delta t) + 2\delta t RHS(t)$$

with X any ocean prognostic variable, δt the timestep and $RHS(t)$ the right hand side of X evolution equation. Timesteps range from typically $\sim 1h$ for ocean climate models to $\sim 10min$ for regional ocean models and $\sim 1min$ for coastal models. The Boussinesq equations are hence solved separately for even and odd timesteps, which requires the addition of the so-called Asselin temporal filter to ensure a convergence between even and odd solutions. Note however that for diffusive terms, the forward Euler scheme is more suitable:

$$X(t+\delta t) = X(t-\delta t) + 2\delta t RHS(t-\delta t)$$

Time and space discretization schemes can be evaluated by estimating the order of their truncation accuracy, that is the behaviour of their error as a function of timestep δt or grid spacing δx. In our case, the leapfrog scheme has 2nd-order accuracy (error of $O(\delta t^3)$), whereas for the forward Euler scheme it is only 1st-order (error of $O(\delta t^2)$).

2.1.2 Space discretization

Ocean model grids are most of the time curvilinear, and rarely unstructured. Unstructured grids permit a more flexible and variable spatial resolution, but with additional numerical costs and a new mathematical formalism. They are used mostly for coastal applications (e.g. tides, surges). Curvilinear grids such as NEMO grid constitute 3D arrays of points with coordinates (i,j,k) oriented along orthogonal directions, one vertical and two horizontal. Horizontal directions do not strictly follow longitude and latitude (Fig.2.1), which permits to position the poles over continents and to avoid the numerical cost of resolving a singular point at the North Pole. NEMO grid is tripolar, with one pole over Eurasia, one over America and one in the Antarctic (Fig.2.1). The i and j directions are not strictly zonal and meridional, so that all operators involving horizontal derivatives in the Boussinesq equations (e.g. ∇, Δ) have to be reformulated. This is however not a crucial issue. Note that each grid cell's surface is specific and is not a simple function of longitude and latitude. As mentioned in Chapter 1, the typical horizontal resolution ranges from $\delta x \sim 100km$ for global climate applications to $\sim 10km$ for ocean-only regional studies and $\sim 1km$ for coastal applications.

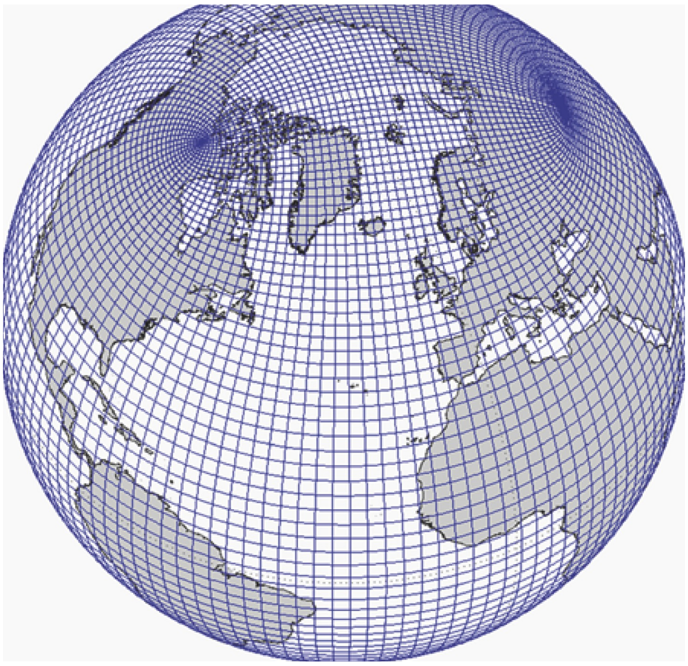

Figure 2.1: NEMO model's tripolar curvilinear grid in the $1/4^{\circ}$ resolution configuration (one every 12 points displayed, source: Madec et al 2016).

Several paradigms exist regarding the definition of oceanic vertical coordinates (Fig.2.2). They can either be truely vertical (so-called z-coordinates), the paradigm being that gravity is the dominant force in the vertical, terrain-following (so-called sigma-coordinates), the paradigm being that the bottom boundary must be continuously defined, or a function of density (so-called isopycnal coordinates), the paradigm being that ocean mixing fundamentally differs along and across isopycnals (isolines of density). Although all arguments are valid, the z-coordinates, mostly used in NEMO, presents the advantage of not impacting the horizontal momentum equations, and in particular not introducing any spurious pressure gradient when iso-level layers are not exactly horizontal. Indeed, all layers in the z-coordinates are at the same depth, with the exception of the bottom cell where a partial cell can be preferred to better reproduce bathymetry. NEMO's z-coordinate has an irregular resolution, higher (typically $\delta z \sim 1-5m$) in the near-surface and lower (typically $\delta z \sim 100-300m$) at depth. Indeed, as we saw in Chapter 1, vertical gradients of oceanic properties are stronger near surface, which requires a higher resolution to represent them. This surface bias of oceanographers can also be interpreted by the larger interest in surface ocean for biological and weather/climate applications and by the lack of knowledge about the abyssal ocean.

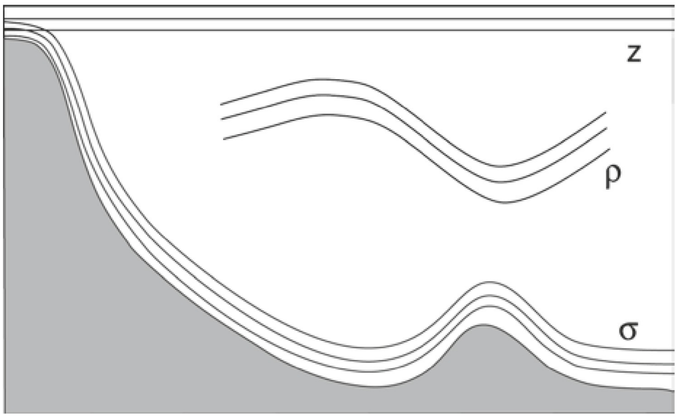

Figure 2.2: Schematic of the three main ocean vertical coordinates in their natural domains of application: vertical z within the mixed layer, sigma σ at the bottom and isopycnal ρ within the interior (source: Benjamin Ménétrier's lecture).

In most ocean models such as NEMO, physical variables are arranged according to the so-called Arakawa C-grid (Fig.2.3). In this grid, scalar variables (θ, S, P, ρ) are located at the center of each cell (in the so-called T-grid), whereas vector variables $(\mathbf{u})$ are located at the center of respectively the eastern, northern and upper faces (so-called U-grid, V-grid and W-grid). This arrangement ensures important conservation properties for scalar variables.

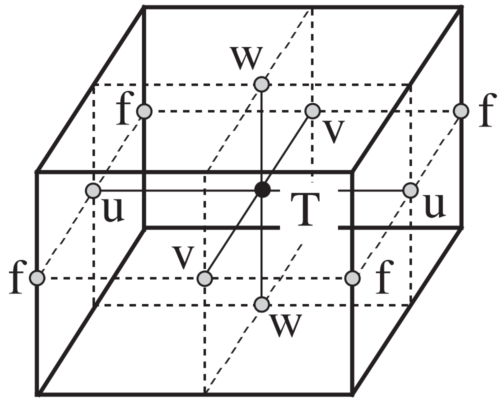

Figure 2.3: *Schematic of NEMO's Arakawa-C grid (source: Madec et al 2016). The location of scalar and vector variables differs by* $1/2$ *gril cell, which ensures important conservation properties for tracers (temperature and salinity).*

A large variety of numerical schemes exists for space discretization. They will not be developed here but it is worth mentioning that they are of crucial importance for the properties of ocean circulation. Typically, climate applications will prefer schemes that conserve integral properties, whereas high-resolution frameworks will privilege schemes that conserve variances and small-scale patterns.

2.1.3 Relation between space and time resolution

A rule of thumb used as a criterion for numerical stability is the so-called "Courant-Friedrich-Lewy" (CFL) criterion. It states that any information should not travel more than one grid cell in one timestep:

$$U\delta t < \delta x$$

with U either the wave or advective velocity. Hence for a typical climate ocean model of timestep $\delta t \sim 1h$ and resolution $\delta x \sim 100km$,

$$U < \frac{\delta x}{\delta t} \sim 20m/s$$

External gravity waves of phase speed $c_g \sim 200m/s$, which are allowed by the equation of sea level η, would cause numerical instabilities for low resolution ocean models. Dividing the timestep by an order of 100 would remove this instability, but it is too costly for long-term modelling and as noted in Chapter 1, the resolution of external gravity waves is not crucial to ocean circulation. Hence two solutions exist: either filtering the fastest waves or splitting the timestep into a long timestep $\delta t_1 \sim 1h$ for the slow 3D (interior) dynamics and a quick timestep $\delta t_2 \sim 1min$ for the fast 2D (depth-integrated) dynamics. The latter option requires an appropriate communication between the slow and fast dynamics.

2.2 Physics

As noted in the former section, most of the physical specifics of oceanic circulation enter through the diffusive closure of turbulence. Because of gravity, the magnitude and the physics behind lateral and vertical exchanges highly differ, which is why horizontal and vertical turbulent diffusivities are defined separately.

2.2.1 Lateral physics

Lateral exchanges are enhanced in the ocean because no work is required against the buoyancy (or gravity) force. They are believed to be dominated by the stirring of oceanic properties by quasi-geostrophic mesoscale eddies. Having said that, it is fair to say that little is known about the actual level of horizontal mixing by mesoscale eddies and the value chosen by modellers responds to numerical stability constraints. Indeed, horizontal mixing operators and coefficients must be tuned to prevent any numerical instability to develop at the small scale, while at the same time not smooting too much the fine-scale oceanic structures. The approach usually slightly differs between tracer and momentum horizontal diffusion:

- Mesoscale eddies are known to stir tracers (θ, S) along isopycnals, rather than along horizontal surface. Hence they have no direct effect on the density of water masses, apart from systematic densification induced by mixing (cabbeling). The horizontal Laplacian operator is therefore slightly rotated to include vertical components and to follow at each grid cell isopycnal surfaces. Note that $\kappa_{hT} = \kappa_{hS}$ because there is no physical rationale for mesoscale eddies to stir differently heat from salt. Typically, we have $\kappa_{hT} \simeq 100m^2/s$ for a global model, but this value should decrease with increasing resolution as mesoscale eddies start being explicitely resolved.
- Resolving small-scale dynamical structures is crucial because most of the ocean kinetic energy is known to lie at the mesoscale. Hence a bilaplacian horizontal operator $\Delta_h^2 = \frac{\partial^4}{\partial x^4} +$

$\frac{\partial^4}{\partial y^4}$ is preferred: it is more scale-selective, so that it permits smaller dynamical structures for a given resolution. Note that correspondingly, κ_{hu} is expressed in m^4/s.

Regarding tracers, a non-diffusive parametrization is added to account for the fact that mesoscale eddies restratify the ocean, which is not accounted for by a diffusive operator. Indeed, they are mostly formed by baroclinic instability which is known to extract gravitational potential energy from the ocean (and atmosphere). A suitable parametrization of this effect is the addition of so-called "eddy-induced velocities" $\mathbf{u_{EIV}}$, which are additional advection terms only applying to tracers and proportional to the local baroclinicity (lateral density gradients).

Finally, lateral boundary conditions must be specified for both tracers and momentum. For tracers, to a very good approximation (neglecting geothermal fluxes), no lateral exchanges occur at the boundary with solid Earth. For momentum, there is no normal flow at lateral boundaries, but the condition on tangent flow is more challenging to determine. Indeed, at the border with solid Earth, there is no tangent flow either, but over a discretized grid this flow is defined over a cell of typically $\sim 1-100km$ width where significant flow can still occur. In practice, this boundary condition is chosen within a continuum between no-slip (no tangent flow at the last grid cell) and free-slip (no slowdown of the tangent flow at the last grid cell), either throughout the domain or changing spatially. This numerical consideration with little physical rationale has tremendous consequences for ocean circulation, especially for transports across straits.

2.2.2 Vertical physics

At the small scale, turbulence occurs over all three directions of space, but because of gravity, the gradients of physical properties are mostly vertical. Hence we only include the impact of this small-scale turbulence on vertical exchanges through vertical diffusivity coefficients. The core of vertical physics in an ocean model is the parametrization of turbulence, a general theoretical framework giving the values of diffusivities as a function of the large-scale (resolved) structure of the flow. Although a variety of models are used for turbulence, the most common within the NEMO community is the so-called Turbulent Kinetic Energy (TKE) scheme. The principle is to resolve a simplified prognostic equation for the turbulent (unresolved) kinetic energy $\overline{\mathbf{u}'^2}$ and to assume that vertical turbulent diffusivities scale with it. More precisely:

$$\begin{aligned} \kappa_{zu} &\propto l\sqrt{\overline{\mathbf{u}'^2}} \\ \kappa_{zT} = \kappa_{zS} &= \frac{\kappa_{zu}}{Pl} \end{aligned}$$

with l a vertical mixing length scale and $1 < Pl < 10$ the variable Prandtl number determining by how much momentum vertical exchanges are larger than those for tracers. Once again, eddy diffusivities are assumed equal for heat and salt. Without detailing the prognostic equation for $\overline{\mathbf{u}'^2}$ (which is hence a new variable of the equation system), we can mention that vertical shear $\frac{\partial \mathbf{u_h}}{\partial z}$ is always a source of turbulence while vertical stratification $\frac{\partial \rho}{\partial z}$ can either be a source (if unstable) or a sink (if stable). Note also that external gravity wave breaking is included as a surface source of turbulent kinetic energy, as are internal waves breaking in the mixed layer through an additional source distributed within that layer.

In the case of static instability, convection should efficiently mix water masses until static stability is restored. However, convection is not allowed explicitely by the hydrostatic nature of the Boussinesq equations. Hence a specific and very simple convection scheme is added in that case. It is named the Enhanced Vertical Diffusion (EVD) scheme, and indeed when static instability occurs:

$$\kappa_{zT} = \kappa_{zS} = \kappa_{zu} \simeq 10m^2/s$$

so that within a few hours of simulation, stability is restored.

In the interior ocean, where the turbulence is weak and convection is absent because of weak shear and/or high stratification, all diffusivities fall down to a background value, typically $\kappa_{zT} = \kappa_{zS} \simeq 10^{-5} m^2/s$ and $\kappa_{zu} \simeq 10^{-4} m^2/s$. Those constant diffusivities also respond to numerical stability constraints and they are far from being physical. They rather reflect the poor knowledge of oceanographers about turbulent processes inducing mixing in the abyssal ocean. However, a few more physical parametrizations exist for the abyssal ocean. One is the internal wave-induced mixing parametrization which distributes over the whole water column the mixing resulting from a climatology of internal wave dissipation energy. Its value typically does not exceed $0.01 m^2/s$, so that it is mostly active in the interior quiescent ocean and within the stratified thermocline. Also a minor double diffusion mixing parametrization accounts for the instabilities caused by the different molecular diffusivities of heat and salt in sea water. Those two parametrizations are the only ones that account for differential mixing between salt and heat, so that $\kappa_{zT} \neq \kappa_{zS}$.

Finally, a bottom boundary condition is needed. For tracers, as in the lateral boundaries, a no flux condition is imposed at the boundary with solid Earth. For momentum, a relatively minor bottom friction can be added, which is a function of an internal wave (mostly tidal) dissipation climatology.

2.3 Surface forcing

In the vertical, another boundary condition is needed, which concerns momentum, water/salt and heat fluxes at the surface (Fig.2.4). Those fluxes include exchanges with the atmosphere, sea ice and river runoff and they have been extensively described in the previous chapter. We will only describe here their specificities in ocean models. First only the solar heat flux Q_{SW} and the river runoff R (and ice shelves/iceberg melting in few configurations) are usually penetrative fluxes, the former with an exponential decay and the second applying evenly over typically $\sim 30m$. All other heat, water fluxes and the turbulent momentum flux (wind stress) only apply to the first model level. Usually, vertical diffusivities are large in the first levels that define the mixed layer, so that those surface fluxes are in practise very rapidly redistributed over the mixed layer depth. But below typically $50m$ depth, the ocean overwhelmingly does not feel directly surface fluxes. In NEMO, surface momentum fluxes are considered as a surface boundary condition of vertical turbulent fluxes:

$$-\rho_0 \overline{w'(0)\mathbf{u_h}'(0)} \simeq \rho_0 \kappa_{zu} \left. \frac{\partial \mathbf{u_h}}{\partial z} \right|_0 \rightarrow \tau_0 = \rho_a C_d |\mathbf{U(10m)}| \mathbf{U(10m)}$$

On the contrary, heat and water forcings are imposed as external sources $\dot{\Theta}$ and $\dot{S}$ for temperature and salinity:

$$\begin{aligned} \dot{\Theta}(z) &= \frac{1}{\rho_0 c_w \delta z} Q_{tot}(z) = \frac{1}{\rho_0 c_w \delta z} (Q_{SW}(z) + Q_{LW} + Q_S + Q_L) \\ \dot{S}(z) &= \frac{1}{\rho_0 \delta z} (E - P - R(z)) \end{aligned}$$

Regarding turbulent air-sea fluxes, several formulations exist depending on the desired applications (Fig.2.4). In coupled mode, there is a continuous feedback between the ocean and atmosphere at the coupling frequency (typically a few hours), so that fluxes at the interface are consistent between both components. In the forced oceanic mode, turbulent fluxes can either be computed from surface atmospheric parameters (so-called "Bulk form") or taken as an external forcing from the atmosphere (so-called "flux form"). A major issue with both strategies is that the ocean has more inertia than the atmosphere, so that the atmosphere should respond quickly to any air-sea flux, which is only possible in coupled mode. We have just stated that the forced oceanic configuration is an ill-defined problem compared to the forced atmospheric one. Hence even in the forced mode, some atmospheric feedback must be accounted for. The advantage of the "Bulk form" is that the feedback is implicit: once the sea surface temperature has changed, surface fluxes will adjust because they are explicitely calculated. On the contrary, the "flux form" does not include any explicit feedback, so that the imposed fluxes could potentially heat or cool the ocean forever. This could lead to unphysical situations. This is why a sea surface temperature (SST) restoration is usually added to surface fluxes in the "flux form" forcing, which mimics the coupling and ensures reasonable temperatures. We use a Newtonian damping so that:

$$Q_{tot} \to Q_{tot} + \alpha_r (SST - SST_{ref})$$

with $\alpha_r \sim -50W/m^2/°C$ the restoration factor and SST_{ref} a reference SST. However, the question of which SST_{ref} to use arises, and no satisfactory solution exists. This is why the "Bulk form" is usually preferred. It is fair to mention that the "Bulk form" also has major limitations: fluxes are computed from temporal averaged atmospheric parameters (typically a few hours), which can induce large errors because fluxes are nonlinear (the average flux is not the flux deduced from averaged parameters); and the "Bulk" formulas used might differ from those of the atmospheric forcing model, which causes an inconsistency between both models. To conclude, coupled modelling is always preferrable for oceanic applications, which is a paradox because most of the ocean modelling community works with ocean-only models. The reason for that is the obvious difficulty to handle a coupled system for an oceanic (or atmospheric) modeller.

We can finally mention two types of ocean modelling frameworks: the so-called "hindcast mode" and the so-called "historical mode". The "hindcast mode" uses an atmospheric hindcast as the forcing, so that the historical chronology of past events is contained in the assimilated atmospheric forcing. There is a chance that due to that, the ocean reproduces the chronology of past events, although a large part of ocean variability is also chaotic and not related to atmospheric forcing. On the contrary, the "historical mode" uses a free atmospheric model only forced by historical anthropogenetic concentrations of greenhouse gases (and sometimes aerosols) as the forcing. In that case the general global warming trend can be reproduced, but no historical chronology is expected to be reproduced because no observation has been assimilated in the atmospheric forcing.

2.4 Model error and ensemble numerical simulations

So far, we have encountered diverse sources of error inherent to ocean modelling:

- Errors related to the approximations of the Boussinesq equation system;
- Errors due to the closure of turbulence in the Reynolds-averaged framework;
- Time and space numerical discretization errors;
- Errors related to initial conditions and surface forcing.

The nonlinear nature of the oceanic circulation equations actually predicts that any small error will tend to exponentially increase until reaching saturation. This is why the atmospheric and oceanic weather is not deterministically predictable beyond a scale between one week and one season. A means to document the error of ocean models is to perform ensemble simulations. The principle is to sample the various sources of error (typically initial conditions, physics or atmospheric forcing) by performing and ensemble of numerical simulations. This probabilistic framework can be used to: document or reduce errors in weather, ocean and climate predictions; study the chaotic part of ocean variability, which is not directly related to any forcing; interpret

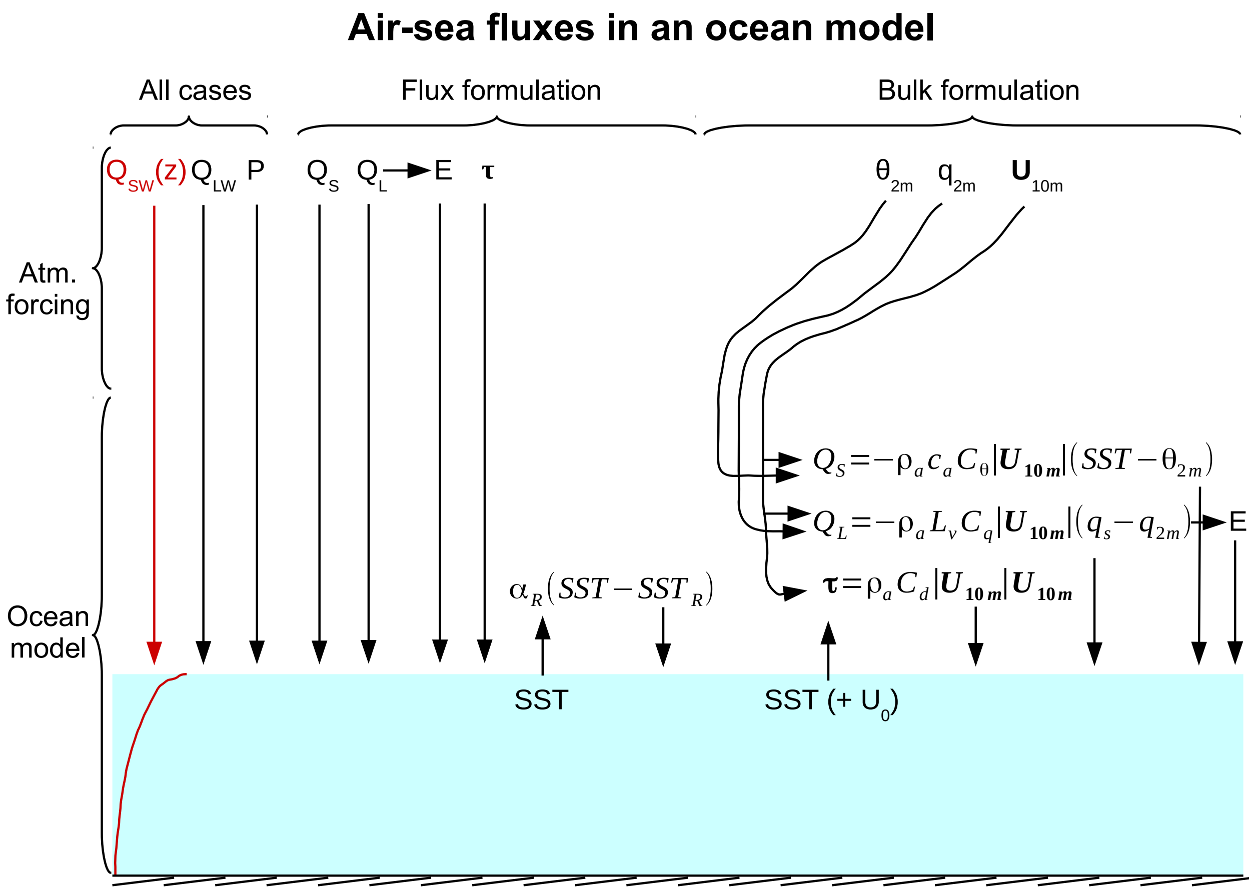

Figure 2.4: Formulation of air-sea fluxes in an ocean model. Radiative fluxes and precipitations are given by the forcing atmospheric model. Turbulent fluxes of heat, water and momentum can either be directly taken from the forcing atmosphere ("flux method") or computed online within the oceanic model ("Bulk method") from the ocean and atmospheric surface parameters (temperature, humidity and wind). The former method usually also includes an SST restoration towards a reference value SST_R (with $\alpha_R < 0$ the restoration coefficient), while the latter method requires to specify which Bulk formulas to use for the computation of turbulent fluxes (to compute C_d, C_θ and C_q).

observations and evaluate more accurately ocean models. It can be considered as a new paradigm for ocean modelling.

2.5 Example 1: 3D configuration of the Mediterranean Sea

Regional ocean models have several specificities with respect to global ones. First, because the domain is reduced, a higher resolution can be afforded. This concerns the physics which can be made eddy-resolving (resolving mesoscale eddies, that is $\sim 1/10°$), the bathymetry which can better resolve channels, straits and interactions with topography, and the atmospheric forcing whose regional features can be made more accurate. In addition, regional domains usually have open boundaries which will have to be specified.

During the tutorials, we will be analyzing the so-called NEMOMED12 model, a regional

NEMO configuration on the Mediterranean Sea (Fig.2.5). It is a semi-enclosed mid-latitude basin where high-resolution regional modelling is required by its key exchanges at narrow straits, key high-resolution atmospheric jets and the need to resolve mesoscale dynamics. Its horizontal resolution is $1/12°$, that is $\sim 6-8km$, it is hence named an eddy-permiting model because it starts resolving mesoscale eddies. Vertical resolution ranges from 1m at surface to $\sim 100m$ at the bottom. The atmospheric flux forcing is a $12km$ resolution regional atmospheric reanalysis covering the period 1979–2013, meaning that observations are assimilated. Hence it is expected that the ocean represents the chronology of past events, and the simulation is qualified as a hindcast run. At its only open boundary with the global ocean, in the near-Gibraltar Atlantic Ocean, θ, S and η are restored towards an oceanic reanalysis and the domain is assumed to be closed. Initial conditions are from an oceanic climatology. Finally, most of the physical options are identical to those presented before.

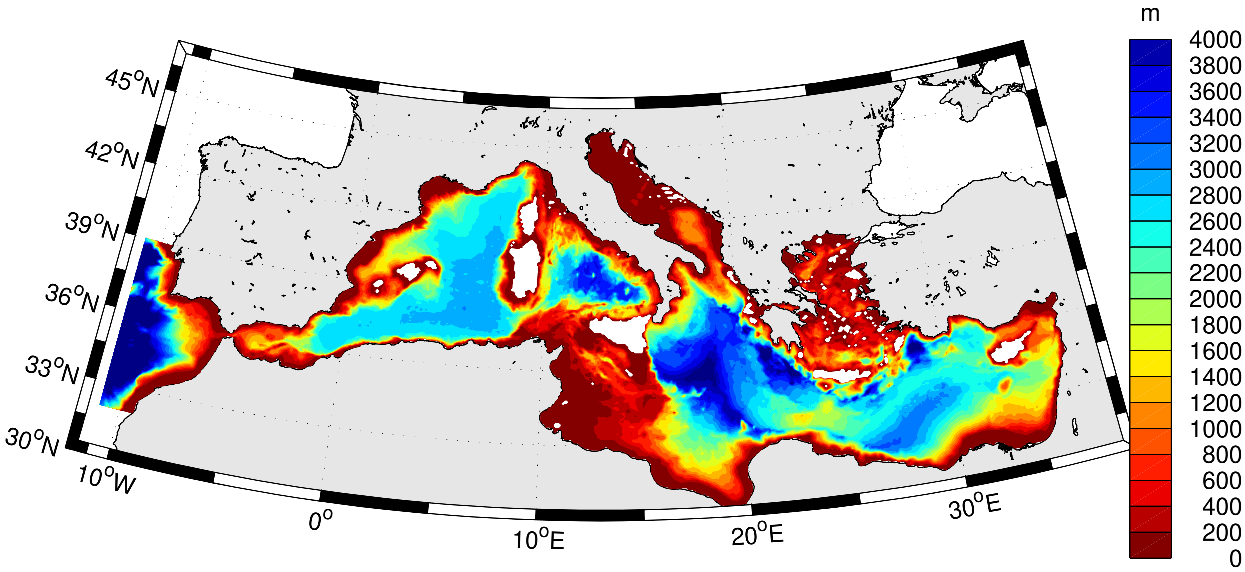

Figure 2.5: *NEMOMED12 domain and bathymetry (source: Waldman et al 2017a).*

2.6 Example 2: CNRM-CM6 global coupled model

2.6.1 General description

CNRM-CM6 model is a global coupled climate model participating in the next Climate Model Intercomparison Programme (CMIP6) in the framework of the International Panel on Climate Change (IPCC) sixth Assessment Report (AR6). It includes the main components of the climate system: ocean, sea ice, atmosphere, continental surfaces and atmospheric aerosols (Fig.2.6). Horizontal resolutions are typically 1° for all components, the vertical oceanic resolution being identical to NEMOMED12 regional Mediterranean model (1m at surface to 200m at deepest levels). We focus here on the historical simulation covering the 1850–2014 period. Its only time-varying external forcings are solar radiations, anthropogenetic greenhouse gases and aerosols (both natural and anthropogenetic) and they follow historical records. An ensemble of 10 members have been run to document the internal climate variability. They only differ in their initial states which come from different years of the control pre-industrial run. This control run has been priorly performed over several hundred years and it ensures a climate equilibration of CNRM-CM6 model under constant pre-industrial external forcings.

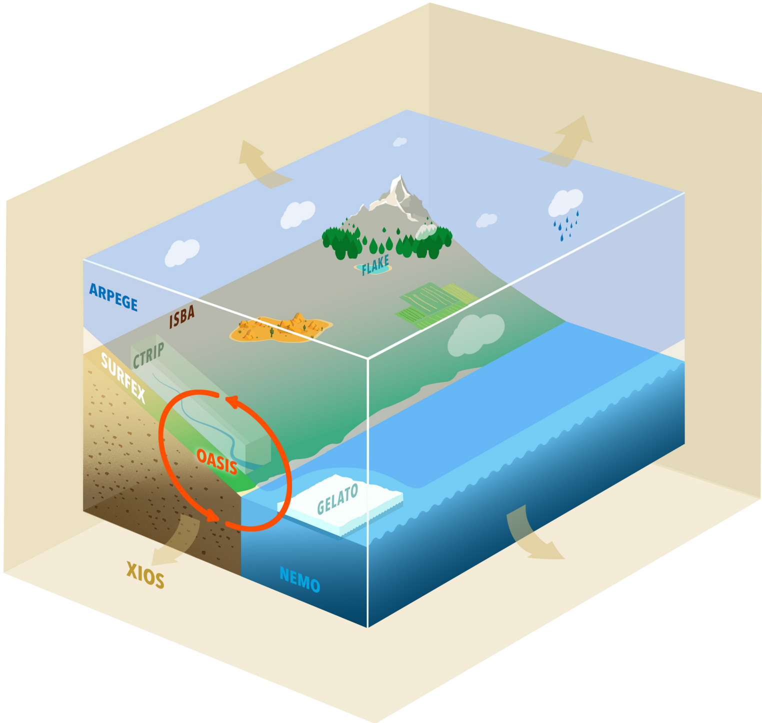

Figure 2.6: *Schematic of CNRM-CM6 coupled model. Its atmospheric component ARPEGE includes an atmospheric aerosol module; its continental surface component SURFEX includes the river drainage module CTRIP, the soil module ISBA and the lake module FLAKE; its oceanic component NEMO includes the embedded sea ice model GELATO; and all components are coupled via OASIS coupler.*

2.6.2 Ocean - Sea Ice component

The ocean component included into CNRM-CM6 is the 1° resolution configuration of NEMO model. Its physical parametrizations are essentially identical to those presented above and to those of NEMOMED12. The only notable difference is the inclusion of the mesoscale eddy-induced velocity parametrization for tracers (temperature and salinity). Indeed, at this resolution, the ocean does not resolve mesoscale eddies at all. Therefore, eddy-induced velocities aim at mimicking the restratification induced by them (see above). The ocean surface is fully coupled with the atmosphere at a 6-hourly frequency using so-called "Bulk aerodynamic formulas", hence no sea surface temperature restoration is required (see above for a discussion on this point).

In addition, and contrary to the regional model NEMOMED12, the coupled climate model includes a sea ice component, GELATO model, fully embededed into the ocean model. It resolves both the sea ice and snow (above sea ice) dynamics and thermodynamics, including their exchanges with both the atmosphere and ocean. Prognostic variables are the sea ice and snow volume and enthalpy, the snow density and the sea ice surface, salinity and age. Hence over each oceanic grid cell, a fraction between 0 and 1 of sea ice area covered with snow is present. Their properties evolve in time as a function of the sea ice interaction with atmosphere and ocean, its transport and vertical heat exchanges.

2.7 Example 3: 1D configuration at the PAPA buoy

Single column models are relevant configurations to test the behaviour of vertical physics parametrizations without adding the complexity of their interaction with horizontal dynamics. It is generally a compulsory step before implementing new vertical physics into a three-dimensional model. In the equations of motion, all horizontal gradients are assumed null, so that lateral advection, turbulent diffusion and vertical advection are removed. This leads to a much simplified set of equations:

$$
\begin{aligned}
\frac{\partial u}{\partial t} - fv &= \frac{\partial}{\partial z}(\kappa_{zu}\frac{\partial u}{\partial z}) \\
\frac{\partial v}{\partial t} + fu &= \frac{\partial}{\partial z}(\kappa_{zu}\frac{\partial v}{\partial z}) \\
\frac{\partial \theta}{\partial t} &= \frac{\partial}{\partial z}(\kappa_{zT}\frac{\partial \theta}{\partial z}) + \frac{1}{\rho c_w}\dot{\Theta} \\
\frac{\partial S}{\partial t} &= \frac{\partial}{\partial z}(\kappa_{zS}\frac{\partial S}{\partial z}) + \dot{S} \\
\rho &= \rho(\theta, S, P_0(z))
\end{aligned}
$$

Horizontal circulation is restricted to Ekman (wind-driven) dynamics, and it only impacts tracers (θ and S) in the fact that the current shear $\frac{\partial \mathbf{u_h}}{\partial z}$ modulates turbulent tracer diffusion κ_{zT} and κ_{zS}.

The most analysed case study is the PAPA buoy located in the subpolar North Pacific off the coast of Canada (Fig.2.7a). In addition to the extensive measurement of oceanic and surface air-sea parameters (Fig.2.7b), it is an area of limited horizontal exchanges where the neglect of horizontal gradients is a reasonable hypothesis. Furthermore, the mixed layer depth presents a significant seasonal cycle, which makes it physically relevant for tests on the vertical physics. In the tutorials, we will analyze the vertical physics of NEMO model on a full seasonal cycle between June 2010 and June 2011.

a) Location

b) Instrumentation

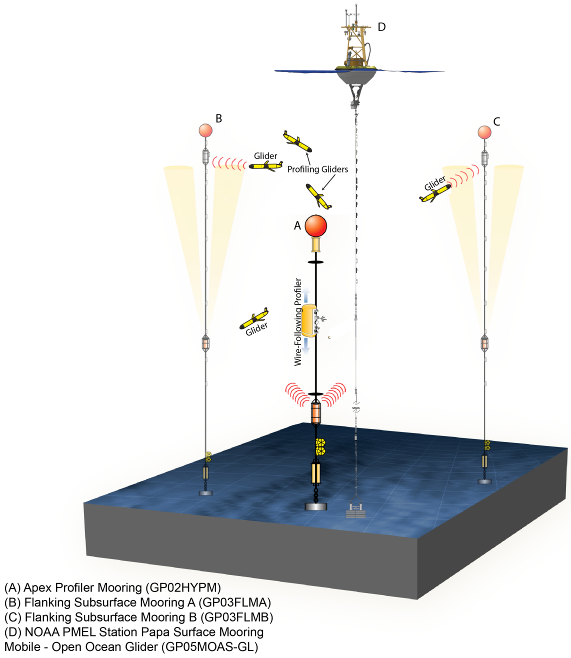

Figure 2.7: Location and instrumentation of the PAPA oceanographic observatory (source: NOAA).

2.8 Practical aspects of numerical modelling

2.8.1 Where do I read the physical description of my run?

In practise, an ocean model is a set of programs, written in a low-level language (e.g. Fortran for NEMO). The core of the model is written in its Fortran routines, and unless specific model development is required, no intervention is needed. Most of the options that users might want to modify are written in a so-called namelist, which is a file specifying the values for the corresponding parameters. Finally, in NEMO model, a set of fundamental options must be specified as compliation keys, in a separate file. Those options are read during the model compilation so that once it is compiled no further change can be made on them. In the tutorials we will briefly analyse the model namelist file.

2.8.2 Grid and mask variables

Because of the curvilinear nature of NEMO grid, a series of elementary grid parameters must be read in a mesh and mask file. In particular, longitudes, latitudes, depths, land-sea masks and scaling factors (δx, δy, δz) are variable at each grid point and differ between the T-grid and the grids for velocities (U-grid, V-grid and W-grid). An important consequence of this is that all space averages should be computed as ponderate means that account for each grid cell's volume, e.g.:

$$< \theta >= \frac{\Sigma \theta \delta x \delta y \delta z}{\Sigma \delta x \delta y \delta z}$$

with $< \theta >$ an arbitrary 3D average. Another consequence, although of lesser importance, is that at a given location (i, j, k), the T-grid can be over the sea while the U-grid (or V-grid) is over land, or vice versa.

2.8.3 Online and offline diagnostics

In numerical modelling, unless no other option is available, online diagnostics are usually preferred to offline ones. Let's illustrate this with the zonal temperature advection term $u\frac{\partial \theta}{\partial x}$. The online diagnostic consists in storing its contribution to the temperature trend during the model computation: hence it is extracted at the model time step, with the model mathematical formulation and numerical scheme for tracer advection. The offline diagnostic consists in trying to retrieve it after the run has already been performed, from the model outputs $\overline{u}$ and $\overline{\theta}$ which are generally stored every month or day. Hence a series of errors are committed: the computation is not done at the model time step, and the mathematical formulation and numerical scheme used might not be identical to those of the model. As a consequence, it is recommended to compute the required physical diagnostics online. However, in practise, one does not always know in advance what physical analysis will be required for a given run, so that some diagnostics have to be performed offline.